Published online: December 17, 2014

Article

TRANSPARENT PROCESS

THE EMBO JOURNAL

The Sm protein methyltransferase PRMT5 is not required for primordial germ cell specification in mice

Ziwei Li[1,2], Juehua Yu[3], Linzi Hosohama[1], Kevin Nee[1,2], Sofia Gkountela[1,2], Sonal Chaudhari[1], Ashley A Cass[4,5,6], Xinshu Xiao[4,5,6] & Amander T Clark[1,2,5,7,*]

Abstract

PRMT5 is a type II protein arginine methyltransferase with roles in stem cell biology, reprograming, cancer and neurogenesis. During embryogenesis in the mouse, it was hypothesized that PRMT5 functions with the master germline determinant BLIMP1 to promote primordial germ cell (PGC) specification. Using a *Blimp1-Cre* germline conditional knockout, we discovered that *Prmt5* has no major role in murine germline specification, or the first global epigenetic reprograming event involving depletion of cytosine methylation from DNA and histone H3 lysine 9 dimethylation from chromatin. Instead, we discovered that PRMT5 functions at the conclusion of PGC reprograming I to promote proliferation, survival and expression of the gonadal germline program as marked by MVH. We show that PRMT5 regulates gene expression by promoting methylation of the Sm spliceosomal proteins and significantly altering the spliced repertoire of RNAs in mammalian embryonic cells and primordial cells.

Keywords conditional knockout; germline absence; PGC specification; PRMT5; splicing

Subject Categories Cell Cycle; Development & Differentiation; Stem Cells

DOI 10.15252/embj.201489319 | Received 18 June 2014 | Revised 1 December 2014 | Accepted 2 December 2014

Introduction

Protein arginine methyltransferase 5 (PRMT5) is a type II arginine methyltransferase that mediates symmetrical dimethylation of arginine (SDMA) in protein substrates. SDMA facilitates interaction with tudor domain-containing proteins, or alternatively can inhibit protein interactions by removing hydrogen bond donors (Bedford & Clarke, 2009). In naïve mouse embryonic stem cells (ESCs), a short interfering RNA (shRNA) knockdown of *Prmt5* results in down-regulation of pluripotency-associated RNAs and up-regulation of differentiation genes (Tee *et al*, 2010). Therefore, PRMT5 is considered an important factor in stem biology where it safeguards pluripotency and prevents differentiation. These same basic principles for PRMT5's mode of action are hypothesized to act during embryo development with the specification of mouse primordial germ cells (PGCs) from the pluripotent epiblast. In this scenario, PRMT5 is hypothesized to function together with the master germline determinant BLIMP1 during gastrulation to repress somatic cell differentiation to promote a germline fate (Ancelin *et al*, 2006).

Although a role for PRMT5 in mammalian PGC specification has not been shown, the precedent for PRMT5 regulating PGC specification comes from work in *Drosophila melanogaster* where a homozygous mutation in the *dart5* gene (the homologue of *Prmt5*) in females leads to progeny that completely lack PGCs (Gonsalvez *et al*, 2006). The underlying mechanism here is hypothesized to involve failed localization of maternal tudor to the pole cells of the embryo, and consequently lack of vasa-positive PGCs (Gonsalvez *et al*, 2006).

PGC specification in *Drosophila* follows the preformation model involving the appropriate localization of RNAs and proteins from the oocyte into the pole cells of the developing embryo, endowing them with PGC fate (for review see Extavour & Akam, 2003). In the mouse, PGC specification follows the inductive model where PGCs are induced between embryonic day 6.0 (E6.0) and E6.5 in the post-implantation epiblast by bone morphogenetic protein 4 (BMP4) and BMP8b signaling (Lawson *et al*, 1991, 1999; Ying *et al*, 2001). BMP signaling induces expression of the transcription factors *Blimp1*, *Prdm14* and *Tfap2c*, which establish the forty founder PGCs at E7.5 at the base of an extra embryonic structure called the allantois (Ohinata *et al*, 2005; Vincent, 2005; Yamaji *et al*, 2008; Weber *et al*,

1 Department of Molecular Cell and Developmental Biology, University of California Los Angeles, Los Angeles, CA, USA
2 Eli and Edythe Broad Center of Regenerative Medicine and Stem Cell Research, University of California Los Angeles, Los Angeles, CA, USA
3 David Geffen School of Medicine, University of California Los Angeles, Los Angeles, CA, USA
4 Bioinformatics Interdepartmental Program, University of California Los Angeles, Los Angeles, CA, USA
5 Molecular Biology Institute, University of California Los Angeles, Los Angeles, CA, USA
6 Department of Integrative Biology and Physiology, University of California Los Angeles, Los Angeles, CA, USA
7 Jonsson Comprehensive Cancer Center, University of California Los Angeles, Los Angeles, CA, USA
*Corresponding author. Tel: +1 310 794 4201; E-mail: clarka@ucla.edu

2010). Mutations in *Blimp1* and *Tfap2c* result in loss of PGCs prior to E8.0 (Ohinata *et al*, 2005; Vincent, 2005). However, a loss of function mutation in *Prdm14* leads to fragile PGCs, which fails to undergo PGC epigenetic reprograming I between E8.0 and E9.25 (Yamaji *et al*, 2008). This global epigenetic reprograming event coined PGC reprograming I occurs simultaneously with a G2 pause in the cell cycle, removal of phosphorylation from serine 2 (Ser2) and Ser5 in the C-terminal domain (CTD) of RNA polymerase II together with genome-wide loss of cytosine methylation and histone H3 lysine 9 dimethylation (H3K9me2) (Seki *et al*, 2005, 2007; Guibert *et al*, 2012; Seisenberger *et al*, 2013). After PGC reprograming I and between E9.25 and E10.5, PGCs undergo a fundamental shift in their developmental program including exit from the G2 pause and phosphorylation of Ser5 and Ser2 in the CTD of RNA polymerase II indicating active transcription and splicing, respectively. Furthermore, PGCs at this stage also migrate into the genital ridges (the site of the future gonad) and express the gonadal-stage germline program represented by mouse vasa homologue (mvh) (Toyooka *et al*, 2000; Kuramochi-Miyagawa *et al*, 2010). From E10.5 to E13.5 PGC reprograming II occurs commensurate with sex determination in the somatic cells. PGC reprograming II involves removal of cytosine methylation from imprinting control centers and single copy genes to establish the germline epigenetic ground state at E13.5 (Hajkova *et al*, 2002, 2008, 2010; Popp *et al*, 2010; Guibert *et al*, 2012; Yamaguchi *et al*, 2012; Vincent *et al*, 2013). The PGC period in mice ends at E13.5 and this is followed by germline differentiation into oocytes or prospermatogonia in females and males, respectively.

Given the fundamental differences between PGC specification in the preformation and inductive models, it is unclear whether PRMT5 will have a conserved role in PGC specification as predicted. In the current study, we used mouse genetics combined with an inducible knockout in mouse embryonic stem cells (ESCs) and PGCs to uncover the role of PRMT5 in mouse germline development.

Results

PRMT5 is dynamically expressed in the mammalian germline

PRMT5 is expressed in the nucleus and cytoplasm of murine PGCs at the time of specification to gonadal colonization before enriching in the cytoplasm of PGCs at E11.5 (Ancelin *et al*, 2006). Using immunofluorescence (IF), we first confirmed previous reports that PRMT5 is localized to the nucleus and cytoplasm of OCT4-positive PGCs prior to E11.5, becoming localized to the cytoplasm of both sexes at E11.5 (arrows, Fig 1A). However, our results show that this is not the conclusion of PRMT5 protein expression. Instead, we discovered that between E11.5 and E13.5 PRMT5 remains expressed in MVH-positive germline cells in the gonad; however, the intracellular localization of PRMT5 depends upon the sex of the embryo. For example, in male PGCs at E13.5, PRMT5 is expressed in the cytoplasm of some cells and in the nucleus of others (Fig 1B), with the formation of bright cytoplasmic PRMT5 foci (Fig 1B insert). From E16.5 to postnatal day 1 (P1) or P2, PRMT5 localizes to both the nucleus and cytoplasm of all prospermatogonia, with discreet cytoplasmic foci that are mostly independent from MVH-positive foci (Fig 1B). In females (Fig 1C), PRMT5 remains in the cytoplasm of germline cells for the remainder of gestation. A summary of PRMT5 localization is shown in Fig 1D.

Male and female PCKO mice are born without germ cells

To address the hypothesis that PRMT5 is required for PGC specification, we generated $Prmt5^{fl/fl}$ mice with *loxP* sites engineered in intron 6 and intron 7 of the *Prmt5* locus (Fig 2A). Recombination between the *loxP* sites resulted in deletion of exon 7, which encodes part of the methyltransferase domain. Unlike the standard *Prmt5* knockout mice which die at implantation (Tee *et al*, 2010), the $Prmt5^{fl/fl}$ mice are viable and fertile. To induce a germline-specific deletion, the $Prmt5^{fl/fl}$ females were bred to *Blimp1-Cre;+ (BC)* transgenic males to generate male and female $Prmt5^{fl/-}$;*BC* (PCKO) mice which were obtained at the expected Mendelian frequency at birth. *Blimp1* is expressed in PGC precursors in the epiblast at E6.25, and the *BC* tool is reported to have 55–75% recombination efficiency in PGCs by E7.5 (Ohinata *et al*, 2005). We evaluated recombination rate at E9.0 and discovered that recombination had occurred in 85% of E9.0 PGCs, and by E13.5 recombination efficiency was 100% (Fig 2B). Analysis of gonads from females and males at postnatal days 1–2 (P1–2) revealed a complete lack of germline cells by histology (male, Fig 2C; female, Fig 2D; arrows in inserts pointing to germ cells). Using IF, we discovered that control (Ctrl) male MVH-positive germ cells and leydig cells express PRMT5 protein in the nucleus (Fig 2E). In contrast, the testes of PCKO embryos had no MVH/PRMT5 double-positive germline cells. Leydig cells, which do not originate from *Blimp1*-positive progenitors, still express nuclear PRMT5. Similar to males, the female PCKO ovaries were also devoid of MVH/PRMT5 double-positive germline cells (Fig 2F; arrows pointing to germ cells).

PGC formation is disrupted between E10.5 and E13.5

To identify the embryonic stage when PGCs are lost, we first evaluated E13.5 embryos and discovered that similar to gonads at birth, both male and female PCKO embryos lacked MVH-positive PGCs in the gonads (Fig 3A and B respectively). Gonad formation was otherwise normal, including formation of seminiferous cords containing SOX9-positive sertoli cells in males (Fig 3A and C). Analysis of E11.5 revealed a small number of PGCs in the genital ridges of PCKO embryos, which were fewer in number compared to the controls (Fig 3D, quantified in G). At E9.5, PGC number and location in the embryo was normal (Fig 3E–G). Morphologically we found that the PCKO embryos at E9.5 were smaller than littermate controls (Fig 3H); however, somite number was within the normal range for E9.5 of development, and embryo turning had occurred indicating that the embryos were not delayed, but rather mildly growth retarded. The growth retardation phenotype of PCKO embryos could be due to a number of factors most likely related to the fact that PRMT5 is also expressed in non-germline cells of the early mouse embryo including the prechordal plate, visceral endoderm as well as Ter119-positive erythroid cells (de Souza *et al*, 1999; Ohinata *et al*, 2005; Vincent, 2005; Wang *et al*, 2007). This growth retardation phenotype was transient, and most PCKO embryos were indistinguishable from controls at E11.5 (Fig 3I). Taken together, our data suggest that PRMT5 is required for PGC survival between E10.5 and E13.5.

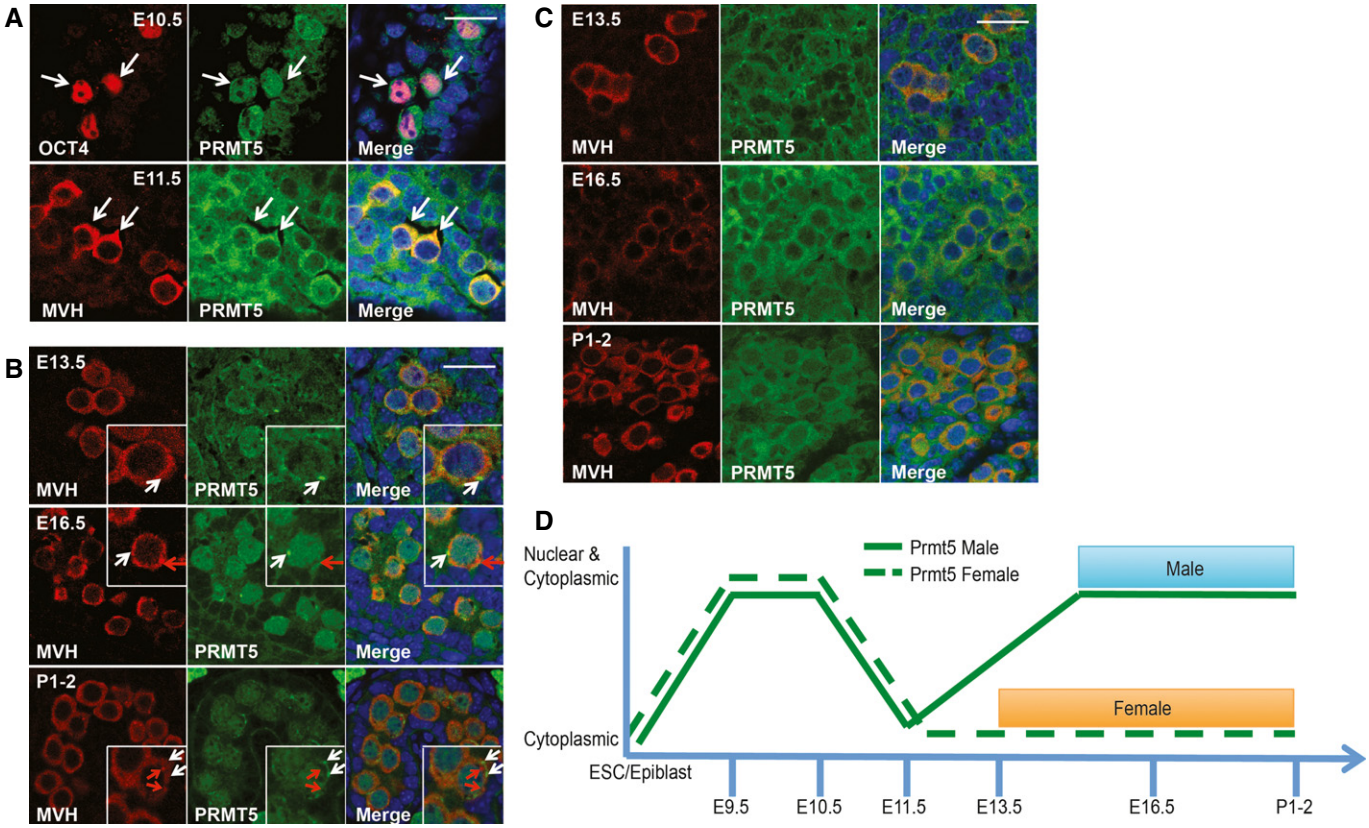

Figure 1. PRMT5 is dynamically expressed in the mammalian germline during embryogenesis.

A IF for PRMT5 (green) and OCT4$^+$ PGCs (arrows) at E10.5, and MVH$^+$ PGCs (arrows) at E11.5 (red).

B PRMT5 (green) in male gonads at E13.5, E16.5 and P1-2. MVH (red) marks germ cells, with PRMT5 foci (white arrow heads) or MVH foci (red arrow heads).

C PRMT5 (green) expression in female gonads at E13.5, E16.5 and P1-2. MVH (red) marks germ cells.

D Summary of expression of PRMT5 in the mammalian germline.

Data information: Two embryos were used in each age. The stainings were performed on wild-type C57BL/6 mice. Scale bar, 20 μm.

PCKO PGCs exit cell cycle and fail to implement the gonadal-stage PGC program

To determine the mechanism by which PGCs are lost in PCKO embryos, we first evaluated apoptosis by cleaved PARP (cPARP) at E10.5 when PGC number is first reduced in the PCKO mutants (Fig 4A). cPARP-positive cells were identified among control and PCKO mutant PGCs as they exited the hind gut; however, an increase in the number of cPARP-positive PGCs were identified in the PCKO embryos (Fig 4A and B). Notably, the migration pattern of PGCs in PCKO embryos was not disrupted indicating that PCKO PGCs are heterogeneously dying in a cell-autonomous manner *en route* to the gonads after E9.5.

The period in germline development between E9.5 and E10.5 represents a major shift in the intrinsic developmental PGC program with exit from the G2 pause, phosphorylation of the CTD of RNA polymerase II, expression of gonadal-stage germline genes and the initiation or reprograming II (Seki *et al*, 2007). To determine whether PGCs in PCKO embryos are still in the cell cycle, we evaluated Ki67 in PGCs at E9.5 and discovered that almost all control PGCs are Ki67 positive and therefore are in cycle (Fig 4C). In contrast, we found that almost half the OCT4-positive PGCs in PCKO PGCs were negative for Ki67 and had therefore had exited the cell cycle (Fig 4C and quantified in D). To evaluate whether PCKO PGCs are no longer in cycle because of a failure to undergo reprograming I, we performed IF for H3K9me2 and 5mC in control and PCKO PGCs at E10.5 and E11.5 (Fig 4E and F). In control PGCs, 5mC and H3K9me2 were depleted from the nucleus (Fig 4E, arrows mark OCT4$^+$ PGCs and F, arrows mark STELLA$^+$ PGCs). This staining pattern is indistinguishable from PCKO PGCs, indicating that loss of 5mC and H3K9me2 had occurred normally in PCKO mutants. To determine whether the gonadal germline program is activated, we evaluated MVH protein which is first expressed in murine PGCs at E10.5 and becomes highly enriched in the cytoplasm at E11.5 (Toyooka *et al*, 2000; Vincent *et al*, 2011). Using IF, we found cytoplasmic localization of MVH in control PGCs at E11.5; however, in PCKO PGCs, MVH protein expression was at background levels in the majority of STELLA-positive PGCs (Fig 4G). Taken together, our data reveal that PRMT5 is required in PGC development but not for PGC specification. Instead, we discovered that PRMT5 is required for the developmental switch that occurs between E9.5 and E10.5 where loss of PRMT5 causes PGCs to exit the cycle and no longer be competent to express MVH protein.

Published online: December 17, 2014
The EMBO Journal

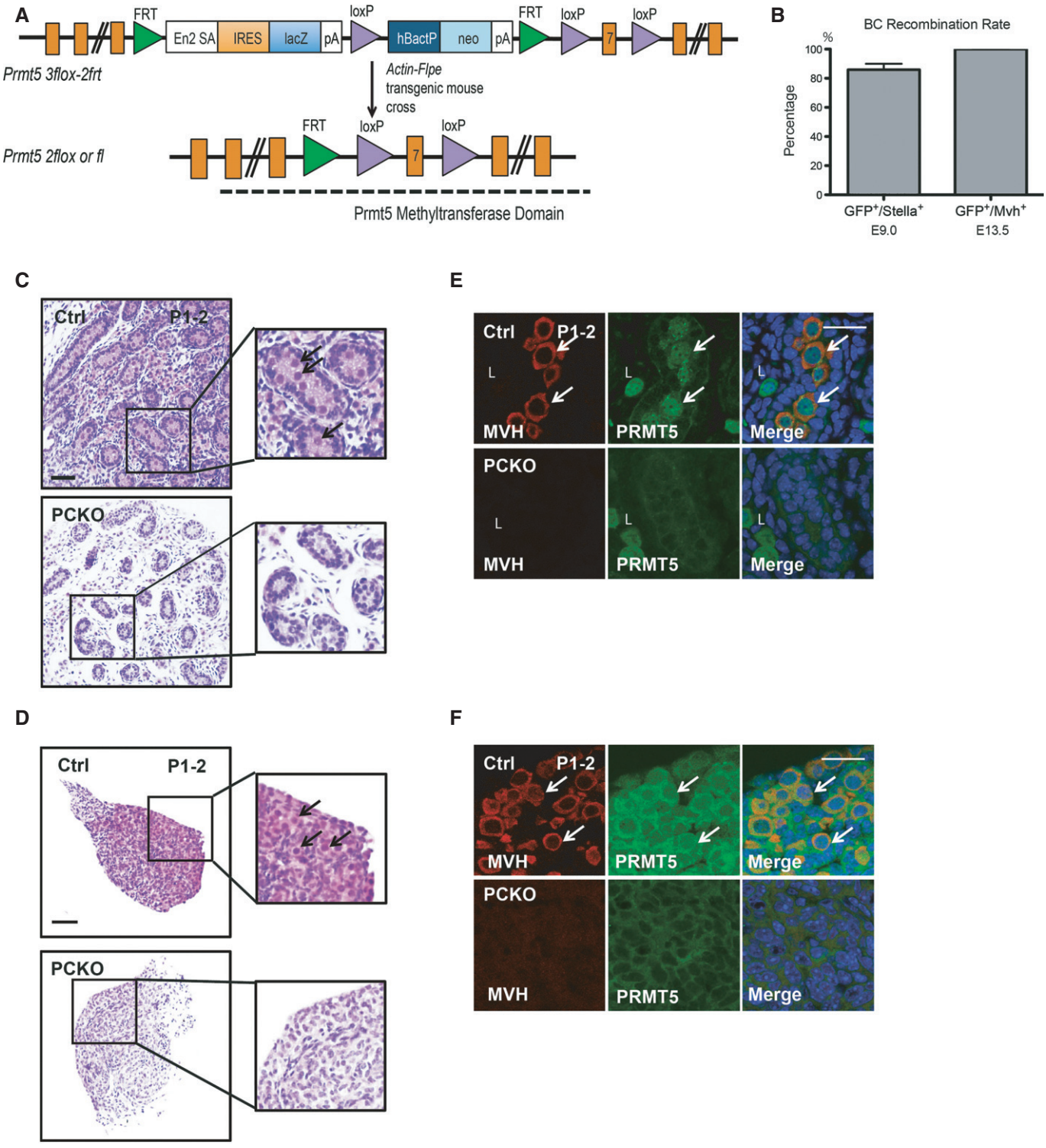

Figure 2. Germ cells are absent in the gonads of PCKO newborn pups.

A Schematic design of the targeting vector. *Prmt5*$^{3flox-2frt}$ founders were mated with *Actin-Flpe* to excise the *FRT* flanked cassette to obtain *Prmt5*^{2flox} or *Prmt5*$^{fl/+}$ mice. *Prmt5*$^{fl/+}$ mice were intercrossed to obtain *Prmt5*$^{fl/fl}$ mice.

B Recombination rate of *Blimp1-Cre* (BC). *BC* was crossed to *YFP lox-stop-lox* mice, and recombination rate was calculated based on the fraction of YFP$^+$ cells in the STELLA$^+$ (E9.0) or MVH$^+$ (E13.5) fraction.

C, D P1-2 male gonad (C) and P1-2 female gonad (D) in control (Ctrl) and PCKO embryos. Arrows indicate germ cells. Scale bar, 100 μm.

E, F IF for PRMT5 (green) and MVH (red) in (E) P1-2 male and (F) P1-2 female gonads. L, Leydig cell. Arrows indicate germ cells. Scale bar, 20 μm.

Data information: Three embryos were used for each sex in each genotype in (C-F). Ctrl: *Prmt5*$^{fl/-}$;+, *Prmt5*$^{fl/+}$;+ or *Prmt5*$^{fl/+}$;*BC*.

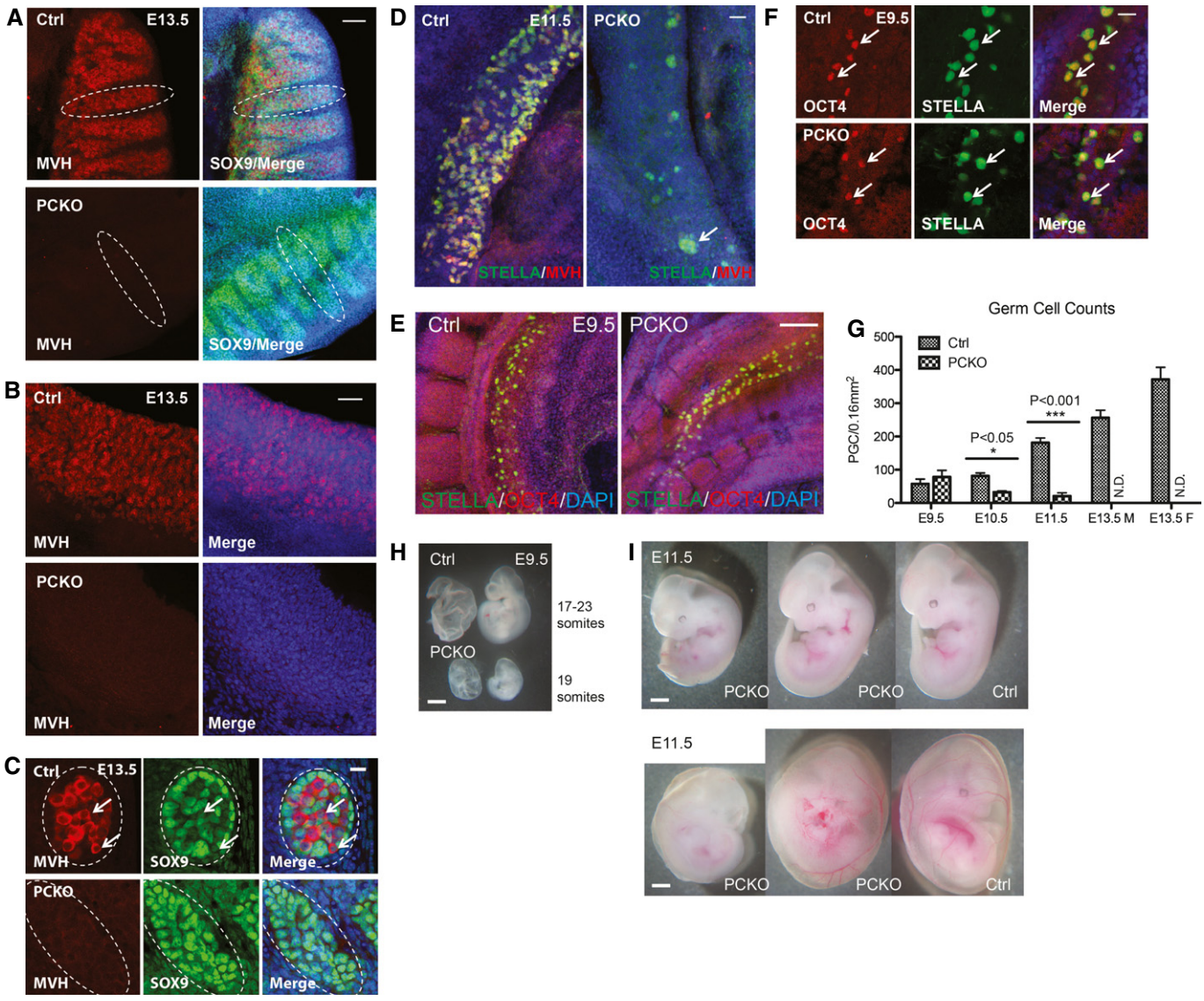

Figure 3. PGCs survival is compromised between E10.5 and E13.5.

A, B IF for MVH$^+$ germline cells (red) in (A) male, and (B) female gonads at E13.5. In males, sertoli cells are also marked with SOX9 (green). Dashed circle indicates a testis cord. Scale bar, 50 μm.

C Higher power image of (A) at E13.5. Dashed circle indicates a cross section through a testis cord. Arrows point to PGCs, which were identified by MVH$^+$ staining. Scale bar, 20 μm.

D IF of the indifferent gonads at E11.5 with PGCs identified by staining for STELLA (green) and MVH (red). Arrows indicate a small PGC cluster in the PCKO mutants. Scale bar, 100 μm. Note that PCKO mutant PGCs are STELLA-positive but not MVH-positive at this magnification.

E IF at E9.5 with PGCs identified by co-staining for STELLA (green) and OCT4 (red). Scale bar, 100 μm.

F Higher power image of (E) at E9.5. Arrows indicate OCT4 and STELLA double-positive PGCs. Scale bar, 20 μm.

G Quantification of germ cell number between control and PCKO at different gestational stages.

H E9.5 embryos from control and PCKO. Scale bar, 1 mm.

I E11.5 embryos of control and PCKO. The majority of PCKO embryos are equivalent size to the control at E11.5. Scale bar, 1 mm.

Data information: Two embryos for each sex in each genotype at E13.5 were used in (A–C). Two embryos of different sexes in each genotype at E11.5 were used in (D). Two E9.5 embryos were used in (E, F). Ctrl: *Prmt5*$^{fl/-}$;+, *Prmt5*$^{fl/+}$;+ or *Prmt5*$^{fl/+}$;*BC*.

PRMT5 regulates gene expression by regulating splicing

To explore the potential mechanism of action, we turned to ground state embryonic stem cells (ESCs) (Ying *et al*, 2008) which have a hypomethylated genome similar to PGCs and express uniform levels of *Nanog, Oct4* and *Sox2* (Ficz *et al*, 2013). To generate ESCs with a conditional knockout, we bred *Prmt5*$^{fl/fl}$ mice to *Rosa26*^{CreERT2} *(CreER)* mice and derived inducible *Prmt5* knockout (iPKO) and inducible *Prmt5* heterozygous (iPHet) ESC lines (Fig 5A). To determine the effectiveness of the inducible system, we added 4-hydroxytamoxifen

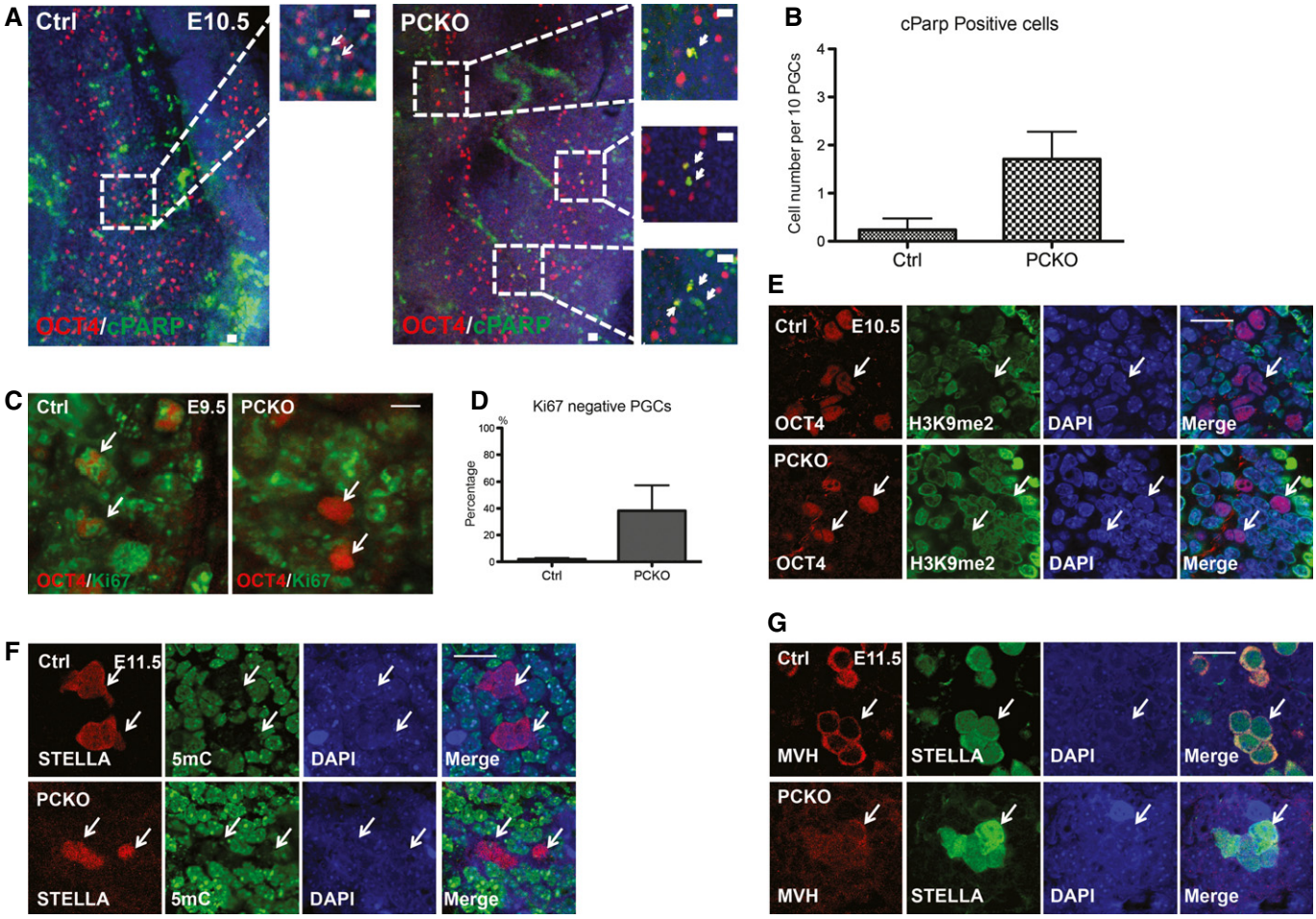

Figure 4. PCKO PGCs exit the cell cycle and fail to progress into MVH-positive PGCs.

A IF of E10.5 embryos showing OCT4$^+$ (red) PGCs with cPARP (green). Arrows indicate apoptotic PGCs. Scale bar, 20 μm.

B Quantification of apoptotic OCT4$^+$ PGCs in control and PCKO embryos at E10.5. Data are shown as mean ± SEM. Standard error is across visual fields containing 10 PGCs. In total, about 4–5 fields were used for the quantification for each genotype.

C IF of E9.5 embryos for Ki67 showing OCT4$^+$ PGCs (arrows). Scale bar, 10 μm.

D Quantification of Ki67 negative OCT4$^+$ PGCs at E9.5. Data are shown as mean ± SEM.

E IF at E10.5 for OCT4$^+$ PGCs and H3K9me2. White arrows mark OCT4$^+$ PGCs. Both Ctrl and PCKO PGCs show the absence of H3K9me2 (green) staining. Scale bar, 20 μm.

F IF at E11.5 for STELLA$^+$ PGCs and 5mC. White arrows mark STELLA$^+$ PGCs. Both Ctrl and PCKO PGCs show the absence of global 5mC (green) staining. Note that STELLA$^+$ PCKO PGCs are not MVH positive at this age. Scale bar, 20 μm.

G IF at E11.5 for PGCs (arrows) with MVH (red) and STELLA (green). Scale bar, 20 μm.

Data information: Two E9.5 embryos, two E10.5 embryos and two E11.5 embryos from each genotype were used in corresponding experiments included in this figure. Ctrl: *Prmt5*$^{fl/-}$;+, *Prmt5*$^{fl/+}$;+ or *Prmt5*$^{fl/+}$;*BC*.

(4-OHT) to iPHet and iPKO ESCs for 2 days and examined PRMT5 expression in nuclear and cytoplasmic fractions using Western blot analysis 5 days after inducing recombination with 4-OHT (Fig 5B). This strategy revealed that exposure to 4-OHT caused loss of PRMT5 protein in the iPKO ESCs relative to iPHet controls.

To determine whether loss of PRMT5 protein caused the mutant ESCs to exit the cell cycle similar to PGCs, we performed Ki67 staining, Western blot for cPARP and counted the total number of cells at days 2, 3 and 5 after plating in 4-OHT (Fig 5B–D). Using IF, we discovered that similar to E9.5 PGCs from the embryo, the majority of iPKO-treated ESCs had exited the cell cycle at day 5 and were negative for Ki67 (red arrows, Fig 5C). In contrast, almost every iPHet-treated control ESC was positive for Ki67 (white arrows). We also found that the iPKO-treated ESCs had increased cPARP (Fig 5B) and reduced growth relative to iPHet controls (Fig 5D). Therefore, a *Prmt5* deletion in ground state ESCs closely resembles the phenotype observed in PGCs in the embryo.

Recent work revealed that a conditional deletion of *Prmt5* in neural progenitor cells (NPCs) caused exit from the cell cycle and apoptosis similar to PGCs and ESCs, with the mechanism due in part to abnormalities in RNA splicing (Bezzi *et al*, 2013). To investigate this in ESCs, we first performed a Western blot using the SYM10 antibody and discovered that SDMA of the core spliceosome proteins SmD1 and SmD3 were reduced in iPKO-treated cells

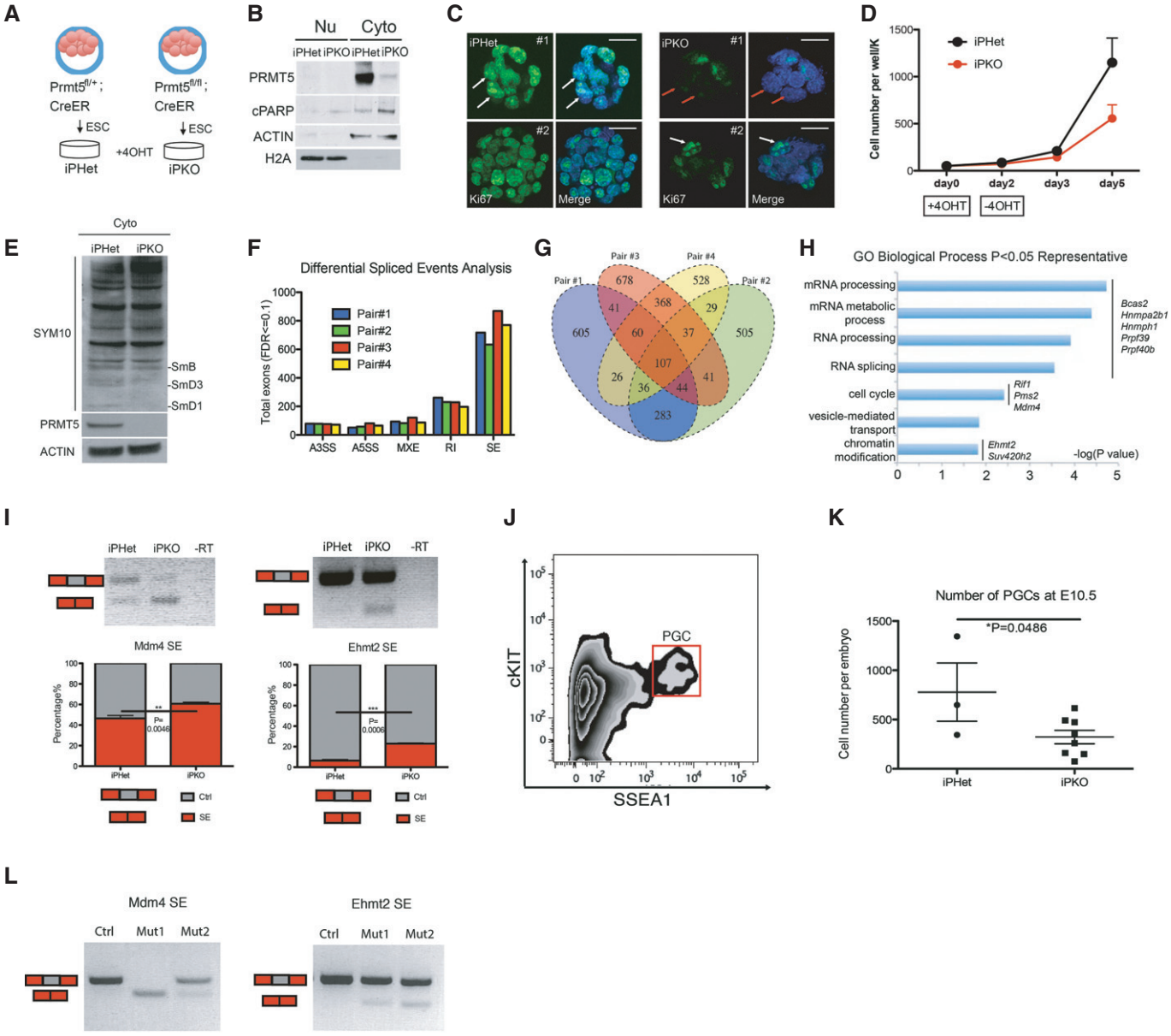

Figure 5. PRMT5 regulates splicing in ground state ESCs.

A Schematic model of ESC derivation. Recombination is induced with addition of 4-OHT in culture for 48 h.

B Western blot of iPHet and iPKO ESCs 5 days after treatment with 4-OHT. Nu, nuclear fraction. Cyto, cytoplasmic fraction. ACTIN and H2A are used for loading control of nuclear and cytoplasmic fraction, respectively.

C IF for Ki67 (green) in iPHet and iPKO ESCs 5 days after treatment with 4-OHT. White arrows mark Ki67-positive ESCs. Red arrows mark Ki67-negative ESCs. Scale bar, 20 μm.

D Growth curve of iPHet and iPKO ESCs at days 2, 3 and 5 after 4-OHT treatment. n = 2 replicates. The original seeding on day 0 is 50,000 (50K) cells per well of a 6-well plate.

E Western blot for SYM10 antibody of iPHet and iPKO ESC cytoplasmic lysates 5 days after treatment with 4-OHT. Cyto, cytoplasmic fraction. ACTIN is used as a loading control. The absence of PRMT5 is shown in iPKO ESCs.

F Pair-wise analysis of differential splicing events in each iPKO replicate relative to the paired iPHet control. A3SS, alternative 3′ splice site; A5SS, alternative 5′ splice site; MXE, mutual exclusive exons; RI, retained introns; SE, skipped exons.

G Venn diagram of pair-wise analysis of MATS, showing overlapping differential splicing events among replicates.

H Representative GO terms for common differentially spliced genes identified in three out of four replicate pairs.

I Reverse transcript (RT) PCR validation of aberrant splicing events in *Mdm4* and *Ehmt2*. SE, skipped exon. PCR is performed among at least three replicates for each locus. Electrophoresis image was quantified using ImageJ software. $^{**}P$ = 0.0046, $^{***}P$ = 0.0006.

J Representative flow plot of sorting cKIT$^+$/SSEA1$^+$ PGCs (red box) at E10.5 using FACS (shown is an embryo with genotype *Prmt5*$^{fl/fl}$;*creER* with 4-OHT injection at E6.5).

K Sorted PGC numbers among control iPHet (*Prmt5*$^{fl/+}$;*creER*) and mutant iPKO (*Prmt5*$^{fl/fl}$;*creER*). $^*P$ = 0.0486.

L PCR validation of aberrant splicing events in *Mdm4* and *Ehmt2* using cDNA reverse-transcribed and amplified from FACS-sorted PGCs (individual embryos) using the NuGEN Ovation RNA Amp System V2. SE, skipped exon. PCR was performed among one control (*Prmt5*$^{fl/+}$;*creER*) and two mutants (*Prmt5*$^{fl/fl}$;*creER*).

compared to iPHet-treated controls (Fig 5E). Given that SDMA of SmD1 and SmD3 are required for generating the spliceosome, a reduction in SDMA suggests problems in RNA splicing. To identify RNA splicing events regulated by PRMT5, we performed paired-end RNA sequencing and used Multivariate Analysis of Transcript Splicing (MATS) on four replicate pairs of iPHet and iPKO ESCs treated with 4-OHT (Fig 5F and G). Using this strategy, we identified > 1,000 abnormal splicing events in the iPKO-treated cells ($P < 0.05$ and FDR < 0.1), with a consistent problem involving exon skipping (SE) (Fig 5F, Supplementary Dataset S1). In order to illustrate the relationships between replicates, we plotted the number of abnormal splicing events in common between paired samples using a Venn diagram (Fig 5G). We discovered 284 overlapping abnormal splicing events in three of the four replicate pairs, with 107 events in common to all four pairs (Fig 5G). This high degree of splicing variability between samples was also observed in the NPC dataset (Bezzi *et al*, 2013) and most likely represents a general instability in RNA splicing in cells with a mutation in *Prmt5*. Using gene ontology analysis, we discovered that abnormally spliced RNAs were enriched in a range of fundamental biological processes including "mRNA processing", "RNA splicing", "cell cycle (which included DNA damage response genes)" and "chromatin modification" (Fig 5H), with some specific examples including abnormal splicing of *Mouse double minute 4* (*Mdm4)* and *Euchromatic histone lysine N-methyltransferase 2* (*Ehmt2*) (Fig 5I). Taken together, our data reveal that PRMT5 functions as a survival factor in PGCs and ESCs with a dramatic effect on splicing of RNAs.

PRMT5 regulates splicing in PGCs

To confirm RNA splicing is also affected in *Prmt5* mutant PGCs, we established timed matings between $Prmt5^{fl/fl}$;*CreER* males and $Prmt5^{fl+}$;*CreER* females, and injected the pregnant females with 4-OHT at E6.5 to induce recombination at the *Prmt5* locus. At E10.5, embryos from the injected pregnant females were harvested, the genital ridges isolated and PGCs sorted from the genital ridges using fluorescence activated cell sorting (FACS) for SSEA1 and cKIT (Fig 5J, red box). Similar to the conditional knockout experiments using *Blimp1-Cre*, inducing recombination at E6.5 with 4-OHT resulted in significantly fewer PGCs in the iPKO embryos compared to the iPHet controls at E10.5 (Fig 5K). By performing PCR using the same primers in Fig 5I, we detected aberrant exon skipping in both *Mdm4* and *Ehmt2* from two independent embryos, respectively (Fig 5L). Therefore, RNA splicing is a common mechanism regulated by PRMT5 in both ground state embryonic stem cells and PGCs.

Discussion

PRMT5 is a dynamic protein required for cellular state and fate. It was previously hypothesized that PRMT5 functions to regulate PGC specification in mice by interacting with BLIMP1 (Ancelin *et al*, 2006). Here, we discovered that PRMT5 does not have a major role (if any) during PGC specification or the subsequent global depletion of 5mC and H3K9me2 from the germline (PGC reprograming I). Instead, we discovered that a germline deletion in *Prmt5* caused the mutant PGCs to exit the cell cycle after specification, with failed expression of the gonadal PGC program marked by MVH. Although our results demonstrate that PRMT5 has a different role to what was previously reported for BLIMP1 in PGC specification, it is still conceivable that PRMT5 works together with BLIMP1, which was not revealed by removal of PRMT5 alone.

The original hypothesis that *Prmt5* is required for PGC specification in mice was made in part by extrapolating results from *Drosophila* (Gonsalvez *et al*, 2006; Anne *et al*, 2007). Given that *Drosophila* uses the preformation model for PGC specification, it is tempting to hypothesize that the lack of an obvious PGC specification phenotype here is due to use of induction to specify PGCs rather than preformation. However, an argument against this hypothesis can be made with the model organism *Caenorhabditis,* which similar to *Drosophila* also uses the preformation mode to specify PGCs (Lesch & Page, 2012). A homozygous *Prmt5* deletion in *Caenorhabditis* results in no obvious PGC specification defect (Yang *et al*, 2009). Instead *Prmt5* mutant germline cells of *Caenorhabditis* are more sensitive to DNA damage by ionizing radiation (Yang *et al*, 2009). Our data indicate that the function of PRMT5 in murine germline development shares similarities to *Drosophila* in that it acts upstream of *vasa* to enable the formation of MVH-positive germline cells. Similarly, the PRMT5 phenotype in mice also shares some similarities with *Caenorhabditis* in that that the germline is sensitive to apoptosis.

A major question extending from these studies is the mechanism by which PRMT5 causes PGCs to exit the cell cycle and be sensitive to apoptosis. Exiting the cell cycle and apoptosis was identified in *Prmt5* mutant ESCs in our study as well as NPCs with a mutation in *Prmt5* (Bezzi *et al*, 2013). This suggests that exiting the cell cycle and failure to survive is a common, and perhaps dominant phenotype in embryonic and progenitor cells that lack PRMT5. PRMT5 is found in a variety of protein complexes where it promotes SDMA (for review see Karkhanis *et al*, 2011). Therefore, it is plausible that PRMT5 has the capacity to simultaneously affect multiple fundamental mechanisms to cause PGC loss, failed ESC growth, loss of NPCs (Bezzi *et al*, 2013) and failed outgrowth of ESCs from murine blastocysts (Tee *et al*, 2010). Given the challenge in working with PGCs from individual mutant embryos between E9.5 and E10.5, we used ESCs as our mammalian cell-based model to show that similar to NPCs a homozygous deletion in *Prmt5* caused depletion of SDMA from spliceosomal Sm proteins, together with abnormal RNA splicing. Although our data do not rule out that other post-translational mechanisms such as SDMA of histones, cell cycle regulators or RNA binding proteins are simultaneously deregulated in *Prmt5* mutant cells, the fact that such a vast array of RNAs have altered splicing indicates that widespread splicing defects are a common feature in mouse cells with a *Prmt5* mutation. Given that PGC survival was not compromised prior to E9.5, our work suggests that PRMT5-dependent splicing is not a major component of PGC development prior to E9.25 (Seki *et al*, 2007). In support of this, PGC reprograming I from E8.0 to E9.25 most likely occurs in the absence of transcription-coupled splicing given the lack of Ser2 phosphorylation on the CTD of RNA polymerase II. Instead, we confirm that PRMT5-dependent splicing is required during the developmental transition from the MVH negative to the MVH-positive gonadal germline program at E10.5.

While this paper was under review, Kim *et al* (2014) discovered that PRMT5 functions to protect genomic integrity by repressing

transposable elements in PGCs during the period when PRMT5 is expressed in the nucleus and cytoplasm up to E10.5. In contrast, our study revealed that PRMT5 acts downstream of the DNA damage response by enabling the correct splicing of primary RNA transcripts involved in RNA processing and the cell cycle including genes that encode for proteins which function in the DNA damage response pathway. These two mechanisms of PRMT5 action, transposon repression and splicing of DNA damage response genes are not mutually exclusive as it is conceivable that de-repressed transposons cause the DNA damage, and a handicapped DNA damage response facilitates the removal of abnormal PGCs from the population through erroneous splicing of RNAs encoding for proteins in the cell cycle and DNA damage response pathway. Indeed, this elegant mechanism, which hinges on the correct function of PRMT5, would ensure and preserve germline quality for the next generation.

In summary, using a combination of stem cell biology and mouse genetics, our work has changed the model for PGC specification in mammals, by revealing that the Sm protein methyltransferase PRMT5 acts after PGC specification to promote PGC survival and correct RNA splicing enabling the transition to an MVH-positive gonadal-stage germline cell.

Materials and Methods

Mouse strains and genotyping

The *Prmt5* knockout first ESCs were obtained from the European Conditional Mouse Mutagenesis Program (EUCOMM; http://www.knockoutmouse.org) and were injected into B6 (Cg)-*Tyr*$^{c-2J}$/J blastocysts (Stock No.000058, The Jackson Laboratory). Male chimeras were backcrossed to C57BL/6J females for germline transmission. To generate the *Prmt5 Flox* allele, the *βgal-neomycin* cassette was removed by crossing *Prmt5* knockout first mice with *β-actin-Flpe* transgenic mice [B6.Cg-Tg(ACTFLP3)9205Dym/J; Stock No.005703, The Jackson Laboratory] to generate *Prmt5*$^{fl/fl}$ mice. 4-hydroxytamoxifen (4-OHT)-inducible knockouts were created by crossing *Prmt5*$^{fl/fl}$ with *Rosa26*$^{CreERT2/CreERT2}$ mice [B6.129-*Gt(ROSA)26Sor*$^{tm1(cre/ERT2)Tyj}$/J; Stock No.008463, The Jackson Laboratory]. At the same time, *Prmt5*$^{fl/fl}$ female mice were crossed to *Blimp1-Cre* [B6.Cg-Tg (Prdm1-Cre)1Masu/J;Stock No.008827, The Jackson Laboratory] male mice to generate male mice with the genotype of *Prmt5*$^{fl/+}$*;BC* (Blimp1-Cre). Germline conditional knockout mice are generated by crossing *Prmt5*$^{fl/+}$*;BC* males with *Prmt5*$^{fl/fl}$ females. For individual experiments, embryos are harvested at E9.5, E10.5, E11.5 and E13.5 with timed-mating strategies. Primers used to identify *Prmt5*$^{fl/fl}$ were *Prmt5*-For: 5′-TTCTTTCTAAGGTGCAGCAGAGGC-3′, *Prmt5*-Rev: 5′-TTGCCTCTTCCTCCTGGTGCTGGG-3′. The mutant band is 371 bp and the wild-type band is 422 bp. All other genotyping methods and primers can be found at http://jaxmice.jax.org/index.html.

Embryonic stem cell (ESC) derivation

ESCs were derived as previously described on MEFs in the presence of 0.5 μM PD0325901 inhibitor plus LIF (Markoulaki *et al*, 2008). The male ESC lines PC1 (iPHet) and PC4 (iPKO) were used for the majority of experiments. ESCs were transitioned to ground state conditions and maintained as previously described (Hayashi *et al*, 2011; Hayashi & Saitou, 2013). To induce a deletion at the *Prmt5* locus, we used 4-OHT (T176, Sigma) at a final concentration of 2 μM for 48 h.

Immunofluorescence

Immunofluorescence was performed on paraffin-embedded sections or by whole mounts of embryos. IF on paraffin was performed as described (Vincent *et al*, 2011). For whole mount, embryos were fixed in 4% PFA for 1 h, permeablized in 1% Triton, and blocked in 10% donkey serum or FBS in PBS with 0.2% Triton. Antibody incubations and washes were performed in 1% donkey serum or FBS in PBS with 0.2% Triton with both primary and secondary antibody incubations occurring overnight. After washing, embryos are cleared in 50% glycerol before mounting in glycerol mounting media on glass slides. Images were taken and processed using a Zeiss LSM780 confocal microscope and Zen2011 software. The primary antibodies used for IF (dilution 1:100) are as follows: Ki67 (556003, BD Pharmingen), PRMT5 (07405, Millipore), OCT4 (sc8628, Santa Cruz), MVH (AF2030, R&D Systems), SOX9 (ab5535, Millipore), STELLA (sc67249, Santa Cruz), 5mC (AMM99021, Aviva Systems Biology), H3K9me2 (ab1220, Abcam), GFP (GFP-1020, Aves Labs) and cPARP (5625, Cell Signaling). The secondary antibodies used (1:400) include donkey anti-rabbit Alexa488, Alexa594; donkey anti-mouse Alexa488; donkey anti-goat Alexa594 (Jackson Immunoresearch).

Western blot

Protein fractions were isolated using the QProteome Cell Compartment Kit (Qiagen) according to manufacturer's instructions. Protein was quantified using the BCA Kit (Thermo), analyzed by electrophoreses on 12% NuPAGE Novex Bis-Tris gels (Invitrogen) and transferred to Hybond ECL Nitrocellulose Membrane (GE Healthcare) according to standard procedures. Primary antibodies (1:1,000) were PRMT5 (07405, Millipore), cPARP (5625, Cell Signaling), ACTIN (sc47778, Santa Cruz), H2A (ab18255, Abcam) and SYM10 (07-412, Millipore). Secondary HRP-conjugate antibodies were from Molecular Probes and Santa Cruz, all used at 1:5,000. Blots were developed using ECL Western Blotting Detection Kit (GE Healthcare).

RNA-seq library preparation and bioinformatics analysis

Total RNA extractions from iPHet and iPKO ESCs were performed with Qiagen RNeasy Mini kit using 1–2 million cells. The RNA-seq libraries were prepared using the Illumina TruSeq RNA Sample Preparation kit and 100 bp paired-end sequencing was performed on the Illumina HighSeq 2500. Reads were mapped to the mouse genome (version GRCm38/mm10) using Tophat2 with approximately 35 million mapped reads per sample. To identify differential splicing events, MATS 3.0.6 beta or Python MATS 3.0.8 (Shen *et al*, 2012) was used for counting junction reads. Only significant events occurring in at least three replicates were taken into consideration. Splicing events were labeled significant using the criteria FDR < 0.1. All sequencing data have been submitted to NCBI BioProject at http://www.ncbi.nlm.nih.gov/bioproject/245758 and are available

under BioProject ID PRJNA245758. GO term analysis was performed with the Database for Annotation, Visualization, and Integrated Discovery (DAVID) (Huang *et al*, 2008) using the biological process (BP) pathway.

Fluorescence activated cell sorting

Timed pregnancy experiments were set up using *Prmt5*$^{fl/fl}$*;CreER* males and *Prmt5*$^{fl/+}$*;CreER* females. Pregnant females were injected with 3 mg/mouse 4-OHT at E6.5. At E10.5, embryos were harvested and genital ridges were dissected from the embryos before digesting the genital ridges to single cells with 0.25% Trypsin (Invitrogen) in the presence of 2 U/ml DNase I (Invitrogen) at 37°C for 5 min. Equal volume of Trypsin Inhibitor (1 mg/ml, Invitrogen) was added to each tube and followed by centrifugation at 500 *g*. Cell pellets were re-suspended in 100 μl FACS buffer (1% bovine serum albumin in PBS) and stained with SSEA1-eFluor660 (1:20; #eBioMC-480, eBioscience) and cKIT-PE (1:100; also known at CD117-PE, #553355, BD Biosciences). Sorted PGCs were collected in 350 μl Buffer RLT in RNeasy Micro kit (Qiagen) followed by RNA extraction according to manufacturer's instruction.

Real-time reverse transcriptase (RT)–PCR and MATS validation

Total RNA from iPHet and iPKO ESCs was extracted using RNeasy Mini kit (Qiagen). 1 μg RNA was treated by DNase I (Invitrogen) for 15 min at room temperature followed by addition of 2 mM EDTA and heat inactivation at 65°C for 10 min. Reverse transcription was performed using SuperScript II reverse transcriptase (Invitrogen) according to the manufacturer's instruction. 1 μl cDNA product was used for PCR in each reaction. Total RNA from PGCs sorted from E10.5 *Prmt5*$^{fl/fl}$*;CreER* and *Prmt5*$^{fl/+}$*;CreER* embryos (induced at E6.5 with 4-OHT) was extracted using RNeasy Micro kit (Qiagen) and immediately snap-frozen at −80°C. The extracted RNA was then processed by Ovation RNA amplification system V2 (NuGEN) according to manufacturer's instruction. 10 ng of cDNA was used to perform PCR in each reaction. MATS validation primers were designed using MacVector to distinguish differential splicing events and semi-quantitative PCRs were performed for 40 cycles and analyzed by gel electrophoresis. Gel intensity from each experiment was analyzed by ImageJ software. *Mdm4* For: 5′-TGTGGTGGAGAT CTTTTGGG-3′; Rev: 5′-TCAGTTCTTTTTCTGGGATTGG-3′. *Ehmt2* For: 5′-AACATCGACCGCAACATCACCC-3′; Rev: 5′-ATACTCGCAGA TGAACGTGCCCTG-3′.

Statistics

Statistical significance was calculated using unpaired *t*-test unless otherwise stated. All data are shown as mean ± standard error of the mean (SEM).

Supplementary information for this article is available online: http://emboj.embopress.org

Acknowledgements

The authors would like to thank the UCLA transgenic core for generating founder chimeras, the UCLA BSCRC flow cytometry core for flow and FACS assistance and Dr. Sanjeet Patel for help with mouse ESC derivation. We thank Dr. You Feng, Dr. Steven G. Clarke and Dr. Tracy Johnson for discussion and input for this work. This work was supported by an R01 grant from the NIH (HD058047) awarded to ATC, and the Eli and Edythe Broad Center of Regenerative Medicine and Stem Cell Research at UCLA Innovation award. Ms. Z. Li was supported by a grant from the Chinese Scholar Council. XX is supported by R01HG006264, and AAC is supported by T90DE022734.

Author contributions

ZL performed, designed the experiments and wrote the manuscript. JY performed, designed experiments and performed computational analysis of RNA-seq data. LH performed experiments. KN performed experiments. SG performed experiments. SC performed experiments. AAC designed and performed computational analysis of RNA-seq data. XX designed and performed computational analysis of RNA-seq data. ATC designed experiments, wrote the manuscript and maintained all required institutional compliances for biological safety and animal work.

Conflict of interest

The authors declare that they have no conflict of interest.

References

Ancelin K, Lange UC, Hajkova P, Schneider R, Bannister AJ, Kouzarides T, Surani MA (2006) Blimp1 associates with Prmt5 and directs histone arginine methylation in mouse germ cells. *Nat Cell Biol* 8: 623–630

Anne J, Ollo R, Ephrussi A, Mechler BM (2007) Arginine methyltransferase Capsuleen is essential for methylation of spliceosomal Sm proteins and germ cell formation in Drosophila. *Development* 134: 137–146

Bedford MT, Clarke SG (2009) Protein arginine methylation in mammals: who, what, and why. *Mol Cell* 33: 1–13

Bezzi M, Teo SX, Muller J, Mok WC, Sahu SK, Vardy LA, Bonday ZQ, Guccione E (2013) Regulation of constitutive and alternative splicing by PRMT5 reveals a role for Mdm4 pre-mRNA in sensing defects in the spliceosomal machinery. *Genes Dev* 27: 1903–1916

Extavour CG, Akam M (2003) Mechanisms of germ cell specification across the metazoans: epigenesis and preformation. *Development* 130: 5869–5884

Ficz G, Hore TA, Santos F, Lee HJ, Dean W, Arand J, Krueger F, Oxley D, Paul Y-L, Walter J, Cook SJ, Andrews S, Branco MR, Reik W (2013) FGF signaling inhibition in ESCs drives rapid genome-wide demethylation to the epigenetic ground state of pluripotency. *Cell Stem Cell* 13: 351–359

Gonsalvez GB, Rajendra TK, Tian L, Matera AG (2006) The Sm-protein methyltransferase, dart5, is essential for germ-cell specification and maintenance. *Curr Biol* 16: 1077–1089

Guibert S, Forne T, Weber M (2012) Global profiling of DNA methylation erasure in mouse primordial germ cells. *Genome Res* 22: 633–641

Hajkova P, Erhardt S, Lane N, Haaf T, El-Maarri O, Reik W, Walter J, Surani M (2002) Epigenetic reprogramming in mouse primordial germ cells. *Mech Dev* 117: 15–23

Hajkova P, Ancelin K, Waldmann T, Lacoste N, Lange UC, Cesari F, Lee C, Almouzni G, Schneider R, Surani MA (2008) Chromatin dynamics during epigenetic reprogramming in the mouse germ line. *Nature* 452: 877–881

Hajkova P, Jeffries SJ, Lee C, Miller N, Jackson SP, Surani MA (2010) Genome-wide reprogramming in the mouse germ line entails the base excision repair pathway. *Science* 329: 78–82

Hayashi K, Ohta H, Kurimoto K, Saitou M (2011) Reconstitution of the mouse germ cell specification pathway in culture by pluripotent stem cells. *Cell* 146: 519–532

Hayashi K, Saitou M (2013) Generation of eggs from mouse embryonic stem cells and induced pluripotent stem cells. *Nat Protoc* 8: 1513 – 1524

Huang DW, Sherman BT, Lempicki RA (2008) Systematic and integrative analysis of large gene lists using DAVID bioinformatics resources. *Nat Protoc* 4: 44 – 57

Karkhanis V, Hu Y-J, Baiocchi RA, Imbalzano AN, Sif S (2011) Versatility of PRMT5-induced methylation in growth control and development. *Trends Biochem Sci* 36: 633 – 641

Kim S, Günestogan U, Zylicz JJ, Hackett JA, Cougot D, Bao S, Lee C, Dietmann S, Allen GE, Sengupta R, Surani MA (2014) PRMT5 protects genomic integrity during global DNA demetylation in primordial germ cells and preimplantation embryos. *Mol Cell* 56: 564 – 579

Kuramochi-Miyagawa S, Watanabe T, Gotoh K, Takamatsu K, Chuma S, Kojima-Kita K, Shiromoto Y, Asada N, Toyoda A, Fujiyama A, Totoki Y, Shibata T, Kimura T, Nakatsuji N, Noce T, Sasaki H, Nakano T (2010) MVH in piRNA processing and gene silencing of retrotransposons. *Genes Dev* 24: 887 – 892

Lawson KA, Meneses JJ, Pedersen RA (1991) Clonal analysis of epiblast fate during germ layer formation in the mouse embryo. *Development* 113: 891 – 911

Lawson KA, Dunn NR, Roelen BA, Zeinstra LM, Davis AM, Wright CV, Korving JP, Hogan BL (1999) Bmp4 is required for the generation of primordial germ cells in the mouse embryo. *Genes Dev* 13: 424 – 436

Lesch BJ, Page DC (2012) Genetics of germ cell development. *Nat Rev Genet* 13: 781 – 794

Markoulaki S, Meissner A, Jaenisch R (2008) Somatic cell nuclear transfer and derivation of embryonic stem cells in the mouse. *Methods* 45: 101 – 114

Ohinata Y, Payer B, O'Carroll D, Ancelin K, Ono Y, Sano M, Barton S, Obukhanych T, Nussenzweig M, Tarakhovsky A (2005) Blimp1 is a critical determinant of the germ cell lineage in mice. *Nature* 436: 207 – 213

Popp C, Dean W, Feng S, Cokus SJ, Andrews S, Pellegrini M, Jacobsen SE, Reik W (2010) Genome-wide erasure of DNA methylation in mouse primordial germ cells is affected by AID deficiency. *Nature* 463: 1101 – 1105

Seisenberger S, Peat JR, Reik W (2013) Conceptual links between DNA methylation reprogramming in the early embryo and primordial germ cells. *Curr Opin Cell Biol* 25: 281 – 288

Seki Y, Hayashi K, Itoh K, Mizugaki M, Saitou M, Matsui Y (2005) Extensive and orderly reprogramming of genome-wide chromatin modifications associated with specification and early development of germ cells in mice. *Dev Biol* 278: 440 – 458

Seki Y, Yamaji M, Yabuta Y, Sano M, Shigeta M, Matsui Y, Saga Y, Tachibana M, Shinkai Y, Saitou M (2007) Cellular dynamics associated with the genome-wide epigenetic reprogramming in migrating primordial germ cells in mice. *Development* 134: 2627 – 2638

Shen S, Park JW, Huang J, Dittmar KA, Lu Z-X, Zhou Q, Carstens RP, Xing Y (2012) MATS: a Bayesian framework for flexible detection of differential alternative splicing from RNA-Seq data. *Nucleic Acids Res* 40: e61

de Souza FS, Gawantka V, Gómez AP, Delius H, Ang SL, Niehrs C (1999) The zinc finger gene Xblimp1 controls anterior endomesodermal cell fate in Spemann's organizer. *EMBO J* 18: 6062 – 6072

Tee WW, Pardo M, Theunissen TW, Yu L, Choudhary JS, Hajkova P, Surani MA (2010) Prmt5 is essential for early mouse development and acts in the cytoplasm to maintain ES cell pluripotency. *Genes Dev* 24: 2772 – 2777

Toyooka Y, Tsunekawa N, Takahashi Y, Matsui Y, Satoh M, Noce T (2000) Expression and intracellular localization of mouse Vasa-homologue protein during germ cell development. *Mech Dev* 93: 139 – 149

Vincent SD (2005) The zinc finger transcriptional repressor Blimp1/Prdm1 is dispensable for early axis formation but is required for specification of primordial germ cells in the mouse. *Development* 132: 1315 – 1325

Vincent JJ, Li Z, Lee SA, Liu X, Etter MO, Diaz-Perez SV, Taylor SK, Gkountela S, Lindgren AG, Clark AT (2011) Single cell analysis facilitates staging of blimp1-dependent primordial germ cells derived from mouse embryonic stem cells. *PLoS ONE* 6: e28960

Vincent JJ, Huang Y, Chen P-Y, Feng S, Calvopiña JH, Nee K, Lee SA, Le T, Yoon AJ, Faull K, Fan G, Rao A, Jacobsen SE, Pellegrini M, Clark AT (2013) Stage-specific roles for Tet1 and Tet2 in DNA demethylation in primordial germ cells. *Stem Cell* 12: 470 – 478

Wang D, Zhuang L, Gao B, Shi C-X, Cheung J, Liu M, Jin T, Wen X-Y (2007) The Blimp-1 gene regulatory region directs EGFP expression in multiple hematopoietic lineages and testis in mice. *Transgenic Res* 17: 193 – 203

Weber S, Eckert D, Nettersheim D, Gillis AJM, Schäfer S, Kuckenberg P, Ehlermann J, Werling U, Biermann K, Looijenga LHJ, Schorle H (2010) Critical function of AP-2gamma/TCFAP2C in mouse embryonic germ cell maintenance. *Biol Reprod* 82: 214 – 223

Yamaguchi S, Hong K, Liu R, Shen L, Inoue A, Diep D, Zhang K, Zhang Y (2012) Tet1 controls meiosis by regulating meiotic gene expression. *Nature* 492: 443 – 447

Yamaji M, Seki Y, Kurimoto K, Yabuta Y, Yuasa M, Shigeta M, Yamanaka K, Ohinata Y, Saitou M (2008) Critical function of Prdm14 for the establishment of the germ cell lineage in mice. *Nat Genet* 40: 1016 – 1022

Yang M, Sun J, Sun X, Shen Q, Gao Z, Yang C (2009) Caenorhabditis elegans protein arginine methyltransferase PRMT-5 negatively regulates DNA damage-induced apoptosis. *PLoS Genet* 5: e1000514

Ying Y, Qi X, Zhao GQ (2001) Induction of primordial germ cells from murine epiblasts by synergistic action of BMP4 and BMP8B signaling pathways. *Proc Natl Acad Sci USA* 98: 7858 – 7862

Ying Q-L, Wray J, Nichols J, Batlle-Morera L, Doble B, Woodgett J, Cohen P, Smith A (2008) The ground state of embryonic stem cell self-renewal. *Nature* 453: 519 – 523

Published online: December 17, 2014